

# We are IntechOpen, the world's leading publisher of Open Access books Built by scientists, for scientists

6,900

Open access books available

185,000

International authors and editors

200M

Downloads

Our authors are among the

154

Countries delivered to

TOP 1%

most cited scientists

12.2%

Contributors from top 500 universities



WEB OF SCIENCE™

Selection of our books indexed in the Book Citation Index  
in Web of Science™ Core Collection (BKCI)

Interested in publishing with us?  
Contact [book.department@intechopen.com](mailto:book.department@intechopen.com)

Numbers displayed above are based on latest data collected.  
For more information visit [www.intechopen.com](http://www.intechopen.com)



# Theoretical Studies on Formation, Property Tuning and Adsorption of Graphene Segments

R.Q. Zhang and Abir De Sarkar  
City University of Hong Kong,  
Department of Physics and Materials Science, Hong Kong SAR,  
China

## 1. Introduction

A single graphene sheet is a planar monolayer of  $sp^2$ -bonded carbon atoms arranged on a two-dimensional honeycomb lattice made of hexagonal rings. Graphene is the basic structural element of some carbon allotropes including graphite, carbon nanotubes and fullerenes. Planar polycyclic aromatic hydrocarbons (PAHs) with only benzenoid hexagonal rings can be viewed as fragments of a graphene sheet with the peripheral atoms saturated with hydrogen, and thus provide molecular models of graphene segments. Graphene segments are of paramount importance both from scientific and technological perspectives. Moreover, the PAHs or graphene segments themselves are of great research interest per se, since they are widely found in the residues of domestic and natural combustion of coal, wood, and other organic materials, and their unique electronic properties provide opportunities for novel functionalized nanomaterials and nanodevices (Wu, Pisula et al. 2007). Understanding the mechanism of formation of graphene segments is necessary to control its formation and in turn, to meet its application requirements. In our work, we have elucidated the role played by H during CVD growth of carbon materials (Zhang, Chu et al. 2000) including graphene and diamond. Graphene materials are endowed with a wealth of properties, including luminescence; which has been frequently reported in various CVD Diamond or a-C:H films (Bergman, McClure et al. 1994; Kania and Oelhafen 1995; Rusli, Amaratunga et al. 1995; Bourée, Godet et al. 1996; Liu, Gangopadhyay et al. 1997). Visible photoluminescence (PL) has been observed in carbon nanoclusters embedded in  $\text{SiO}_2$  matrix (Zhang, Bayliss et al. 1996) and from  $\text{C}_{60}$  thin films (Gapozzi, Casamassima et al. 1996). Unlike a-Si:H, the PL efficiency of a-C:H film is high and it shows luminescence even at room temperatures (Wagner and Lautenschlager 1986; Fang 1991; Schütte, Will et al. 1993; Xu, Hundhausen et al. 1993; Nevin, Yamagishi et al. 1994). A clear understanding of the luminescence phenomenon would help to produce high-quality luminescent films by a proper control of the experimental conditions. Correspondingly, the structure property relationship responsible for broadband luminescence in a:C-H films and carbon nanostructures was clearly pinpointed in our work (Zhang, Bertran et al. 1998; Feng, Lin et al. 2009). To the best of our knowledge, size-dependent PL mechanism was first reported by us (Zhang, Bertran et al. 1998).

The intermolecular, weak  $\pi$ - $\pi$  interactions are of utmost importance for understanding the various properties of graphene sheets (Novoselov, Geim et al. 2004; Feng, Lin et al. 2010)

and other carbon-related nanostructures, including hydrogen-terminated graphene nanoribbons with a finite nanosize width (Barone, Hod et al. 2006). The role of  $\pi$ - $\pi$  interactions in benzene dimers (Feng, Lin et al. 2010) and in the stacking of graphene sheets (or graphene multilayers) have been thoroughly addressed in our detailed theoretical studies (Feng, Lin et al. 2009). In our investigations (Lin, Zhang et al. 2007; Fan, Zeng et al. 2009), the weak van der Waal's (vdW) interactions were also found to be of pivotal significance in binding bio-molecules to carbon nanotubes (CNTs) from the viewpoints of important biological applications and bio-compatibility. These non-covalent, weak interactions do not affect the chemical and conductive properties of carbon nanotubes unlike covalent bonds and thereby aid an efficient retention of its pristine properties during their actual practical applications.

Water is a universal solvent and plays a crucial role in the mechanism of a variety of chemical and biological processes. The properties of water molecules or clusters in different ambiances can be a lot different from that of its bulk phase. To shed light on that, we have probed theoretically into the interaction of water clusters with graphite (Lin, Zhang et al. 2005). Single-walled carbon nanotubes (SW-CNTs) have novel structural, mechanical, and electronic properties but are hydrophobic. Water encapsulated within hydrophobic SW-CNTs, commonly known as ice nanotubes (INT), provide important clues to the functionality of biological nanopores (Sansom and Biggin 2001). Moreover, INTs have been found to exhibit novel properties such as proton conduction, hydrogen-bond network, phase transitions, etc (Maniwa, Kumazawa et al. 1999; Hummer, Rasaiah et al. 2001; Koga, Gao et al. 2001; Martí and Gordillo 2001; Noon, Ausman et al. 2002; Mann and Halls 2003; Martí and Gordillo 2003; Mashl, Joseph et al. 2003; Wang, Zhu et al. 2004). Through a systematic investigation, we have revealed the geometrical structure adopted by INTs within SW-CNT and the signatures in its vibrational spectra (Feng, Zhang et al. 2007).

Hydrogen is one of the most promising energy fuels for automobiles and can be potentially exploited in smaller portable devices. Due to the large surface area, carbon-based nanostructures, such as CNTs, appear to be ideal storage materials for the hydrogen storage. There is an ongoing debate within the experimental community with regard to the viability of CNTs as hydrogen storage materials. Our effective predictive modelling (Fan, Zhang et al. 2009) provides important and useful pointers to experimentalists on this. The chapter systematically organizes our computational findings pertaining to graphene segments into different sections, which is intended to provide a deep insight into the properties of graphene segments and useful guidance to future research and applications.

## 2. Graphene synthesis

A scientifically clear understanding of the different methods for graphene synthesis is essential to realize the optimum potentiality of graphene in a large variety of its applications. The size and quality of the graphene produced depends on the techniques used and the next sub-sections are devoted to some of the commonly used methods, their merits and demerits.

### 2.1 Chemical Vapor Deposition (CVD) approach

Synthesis of graphene by CVD has been introduced recently (Sutter, Flege et al. 2008; Li, Cai et al. 2009; Li, Zhu et al. 2009; Reina, Jia et al. 2009; Reina, Thiele et al. 2009). Graphene acquired from the CVD process has demonstrated large area, high quality, controllable

number of layers and low defects. CVD approach has been found to be by far the most effective technique to produce high quality, large scale graphene that can be compatibly integrated into the Si device flows.

The CVD based graphene synthesis process typically involves a thin layer of a transition metal (usually a few hundred nanometers thick) deposited on a substrate e.g. SiO<sub>2</sub>. The substrate is then put into a furnace to be heated up to about 1000° C in a hydrocarbon gas (e.g. methane and hydrogen) environment. The transition metallic layer catalyzes the decomposition of hydrocarbon gas and the dissociated carbon atoms gradually absorbs into the metal layer or diffuses/remains on the metal surface depending on the metal. Experimentally, many different transition metal catalysts, (e.g. Ru, Ir, Pd, Ni, Cu) have been used to synthesize graphene and two distinct growth mechanisms have been proposed (Li, Cai et al. 2009). **(I)** Precipitated growth, in which decomposed C atoms dissolve into the catalyst first and then precipitate to the metal surface to form graphene during the subsequent cooling. This is because the solubility of carbon in the metal decreases with temperature and the concentration of carbon decrease exponentially from the surface into the bulk. The follow-up cooling process helps the carbon atoms to segregate to the metal surface to form graphene. **(II)**. Diffusive mechanism, in which the decomposed C atoms remain or diffuse on the metal surface and then incorporate into graphene directly. Mechanism I corresponds to those metals that interact strongly with C atoms and has the binary phase of metal carbide (e.g., Ni) and growth mechanism II corresponds to those which have no metal carbide phase (e.g., Cu). For mechanism I, continuous precipitation of C from the interior of catalysts normally leads to the non-uniform, multilayer formation of graphene layer as carbon prefers to segregate at the nickel grain boundaries (Yu, Lian et al. 2008). This problem is alleviated in mechanism II (Li, Cai et al. 2009) and it is known to be the best for the synthesis of monolayer graphene. Notably, inch-sized graphene has been demonstrated and synthesized on the Cu foil surface (Li, Cai et al. 2009; Li, Zhu et al. 2009). A rapid cooling rate in mechanism I can aid the suppression of preferential segregation of carbon at grain boundaries of the metal (e.g Ni) and thereby control the number of graphene layers (Kim, Zhao et al. 2009), as demonstrated by Kim *et al.* Graphene segregation during cooling is a non-equilibrium process (mechanism I). Non-equilibrium segregation in general involves the transport of vacancy-impurity (vacancy-carbon in this case) complexes to sinks, such as grain boundaries and surfaces during cooling, and strongly depends on the cooling rate (Thuvander and Andrén ; Yu, Lian et al. 2008). Different cooling rates lead to different segregation behaviors. Extremely fast cooling rate results in a quench effect in which the solute atoms lose the mobility before they can diffuse. A finite amount of carbon is found to segregate at the surface at medium cooling rates, which is found to be optimal. The extremely slow cooling rate allows carbon with enough time to diffuse into the bulk, so there will not be enough carbon segregated at the surface. Roughness of the metal substrates affects the uniformity of graphene layers synthesized by CVD (Yu, Lian et al. 2008). Thinner and more uniform graphene can be synthesized on smoother Ni substrates.

Metal-catalyzed graphene synthesis has been very well studied. Yet, the role of H<sub>2</sub> in the growth atmosphere, which is also very crucial for graphene growth, needs to be addressed duly.

### 2.1.1 Role of H<sub>2</sub> during CVD growth

It is well-known that hydrogen gas plays a key role for CVD diamond growth, while it acts as an etchant for amorphous carbon. A hydrogen molecule is very stable at temperatures up

to 1000 °C. However, in the presence of a metal catalyst, at about 450 °C, the molecule dissociates and becomes reactive. Dissociation of the H<sub>2</sub> molecules in the presence of Ni and other metals was clearly demonstrated in an experiment done by Haluška et al. (Haluska, Hirscher et al. 2004). Atomic hydrogen then acts as an etching agent reducing preferably amorphous carbon that contains unsaturated dangling bonds. The role of etching by hydrogen during CVD is discussed in the following sub-section.

#### 2.1.1.1 Etching by hydrogen during CVD

Diamond deposition with CVD has been successfully demonstrated using hydrogen as an etchant to remove the non-diamond phase. The selectivity of hydrogen in etching the two carbon phases, graphite and diamond, is considered the key factor for success in the synthesis of high-quality diamond films. The preferential etching of the sp<sup>2</sup> phase over the sp<sup>3</sup> phase by atomic hydrogen has been extensively reported. The role of atomic hydrogen both as sp<sup>2</sup> etchant and sp<sup>3</sup> promoter during the diamond growth is therefore well recognized experimentally and theoretically (Loh, Foord et al. 1996; Mendes, Corat et al. 1997). In addition, the etching selectivity of hydrogen has also been used to control the preferential growth orientation for obtaining oriented diamond crystals (Zhang, Jiang et al. 1997). Our comprehensive theoretical study based on Hartree-Fock (HF) molecular orbital approaches (Zhang, Chu et al. 2000) revealed the role of hydrogen species during the CVD growth and clarified the etching effect of the hydrogen species on sp<sup>2</sup> phase of carbon.

The overlap between the Highest Occupied Molecular Orbital (HOMO) of one molecule and the Lowest Unoccupied MO (LUMO) of another (also known as electron delocalization) determines the nature of chemical reaction between the two molecules (Hoffmann 1988; Fukui and Fujimoto 1997). Because the extent of electron delocalization is inversely proportional to the energy difference between these MOs, a small energy difference between the HOMO of one molecule (electron donor) and the LUMO of the other (electron acceptor) indicates a favorable reaction. This energy difference between HOMO of the electron donor and LUMO of the electron acceptor is hereafter referred to as the HOMO–LUMO difference of the reacting system. The frontier orbitals (HOMO and LUMO) were determined in this work using HF and configuration interaction (CI) instead of density functional theory (DFT) because the latter theory provides too close occupied and unoccupied states to analyze.

Under typical CVD conditions of diamond growth, hydrogen exists as various species of neutrals and ions. The HOMO-LUMO difference (with hydrogen as electron donor) as a function of the cluster size of two types of clusters is shown in Fig. 1. Each curve displays an overall tendency to decrease as the cluster size increases. This result is consistent with our earlier report (Zhang, Bertran et al. 1998) that the HOMO-LUMO gap of the same silicon or carbon cluster decreases as the cluster size increases and levels off when the cluster size reaches about 30 atoms. Thus, the reactivity of hydrogen species is less sensitive to the cluster size for larger clusters. The HOMO-LUMO differences between neutral hydrogen and all the clusters are illustrated in Figure 1(a), in which molecular hydrogen shows larger HOMO-LUMO differences and thus exhibits a lower reactivity than the atomic hydrogen. This relatively low reactivity of molecular hydrogen gives rise to the well-known small etching effect of molecular hydrogen in CVD processes (Harris, Doll et al. 1995). Being an abundant species in some CVD processes, atomic hydrogen is considered to act as the phase etchant. As illustrated in Figure 1(a), the HOMO-LUMO difference of H/sp<sup>2</sup>-carbon is significantly different from that of H/sp<sup>3</sup>-carbon, indicating that the reactivity of atomic hydrogen with the two carbon phases should be considerably different. The smaller HOMO-

LUMO difference of H/ $sp^2$ -carbon implies the preferential etching selectivity for the  $sp^2$  phase, which is in good agreement with experiments (Donnelly, McCullough et al. 1997; Ishikawa, Yoshimi et al. 1997).

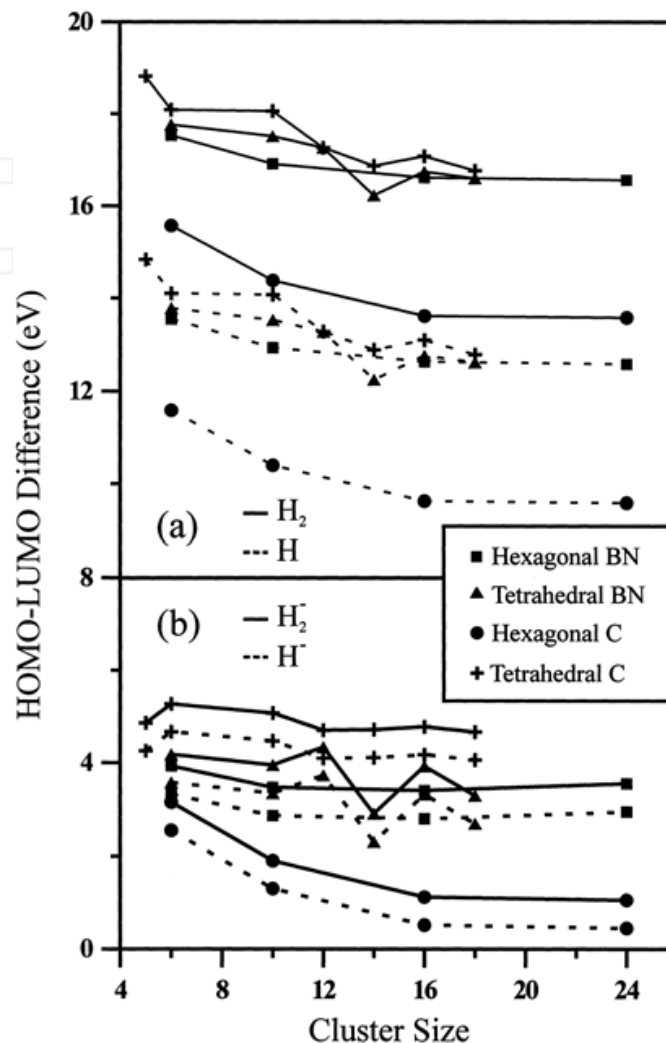


Fig. 1. HOMO-LUMO differences between (a) neutral hydrogen species and (b) negative hydrogen species; and BN, carbon clusters as functions of atomic number (Zhang, Chu et al. 2000).

Fig. 1(b) shows the HOMO-LUMO difference of the  $H^-$  ion and the clusters. The result shows that the reactivity of the  $H^-$  ion is considerably higher than that of the neutral hydrogen. Similar to the case of neutral hydrogen, the  $H^-$  ion shows preferential etching of the  $sp^2$ -carbon over the  $sp^3$ -carbon phase. In fact, when the charged hydrogen ion approaches the carbon clusters, charge transfer may take place. This may lead to neutralization of the  $H^-$  ion and charging of the carbon clusters. Finally, the chemical reaction occurs between the charged clusters and neutral hydrogen. Hence, the reactivity of the hydrogen ion can also be explored from the point of view of charge transfer. Although it is impossible to obtain the HOMO-LUMO data for  $H^+$ , using the concept of charge transfer, the information about  $H^+$  may be indirectly studied by considering the reactivity between positively charged clusters and the atomic hydrogen. Table 1 lists the results on small charged clusters. Comparing with the neutral, the negatively charged cluster has its HOMO

and LUMO moved up. The energy difference between the HOMO of the negatively charged cluster and the LUMO of hydrogen is relatively small, indicating that the reactivity between the charged cluster and hydrogen is still higher than that between neutrals. For the positively charged cluster, the calculated HOMOs and LUMOs move to lower energies. The reactivity of atomic hydrogen (electron donor now) with the positively charged cluster is still higher than that with neutral cluster. Hydrogen ions also found in experiments have a higher reactivity than their neutral one (Davis, Haasz et al. 1987), which is in good agreement with our results.

	HOMO	HOMO of neutral	LUMO	LUMO of neutral
$C_6^+$ (sp <sup>2</sup> )	-0.55619	-0.33067	-0.23272	0.14906
$C_6^+$ (sp <sup>3</sup> )	-0.59758	-0.42311	-0.36760	0.22666
$C_6^-$ (sp <sup>2</sup> )	0.05325	-0.33067	0.36703	0.14906
$C_6^-$ (sp <sup>3</sup> )	0.20480	-0.42311	0.37316	0.22666

Table 1. HOMO and LUMO Values of Small Charged Clusters in Comparison with Those of Neutral Ones, Obtained Using HF Method with Basis Set 6-31G\*\* (Unit: au) (Zhang, Chu et al. 2000).

	HOMO			LUMO		
	carried charge (atomic unit)			carried charge (atomic unit)		
	-1	0	+1	-1	0	+1
$C_6$ (sp <sup>2</sup> )	0.05325	-0.33067	-0.55619	0.36703	0.14906	-0.23272
$C_{10}$ (sp <sup>2</sup> )	0.02096	-0.28689	-0.48896	0.29973	0.10296	-0.20351
$C_6$ (sp <sup>3</sup> )	0.20480	-0.42311	-0.59758	0.37316	0.22666	-0.36760
$C_{10}$ (sp <sup>3</sup> )	0.18870	-0.42209	-0.55917	0.34822	0.21937	-0.33920

Table 2. Trend for HOMO and LUMO with Cluster Size (Unit: au) (Zhang, Chu et al. 2000).

As shown in Table 2, the influence of carried charge on the HOMO and LUMO energies decreases as the cluster size increases. This suggests that charge transfer has only a minor influence on the larger clusters. Accordingly, the charge-transfer effect should have little influence on the conclusions drawn from the calculations for neutral species. We note that while charging might influence the sticking probability of the species with the substrate, the bonding characteristics between the two parties would be mainly determined by the reactivity between their neutrals. The interaction between hydrogen species and the substrate has two meanings: their sticking to the substrate and their chemical reaction with the substrate. The higher reactivity of the hydrogen ion implies a higher sticking probability with the substrate than for atomic hydrogen. In summary, atomic hydrogen and hydrogen ions show a large difference in their reactivities towards the sp<sup>2</sup> and the sp<sup>3</sup> carbon phases. This difference facilitates the diamond growth via CVD methods. Hydrogen ions also show higher reactivity than the neutral.

### 2.1.1.2 Prevention or minimization of etching

The effects of hydrogen can be turned around to the aid of synthesis and growth of graphene during CVD by a careful control of the growth conditions. Despite the etching action of hydrogen on the sp<sup>2</sup> phase of carbon, it is found that a critical amount of hydrogen is necessary to synthesize a few layers of graphene. This is because hydrogen maintains a balance between the production of reactive hydrocarbonaceous radicals and the etching of

the graphene layer during the CVD process. If the ratio of methane to hydrogen is too low, the etching reaction becomes much faster than the formation of graphene layers. This was also experimentally proved in a recent work of Kong's group (Reina, Thiele et al. 2009). As a result, the ratio of gas mixture between methane and hydrogen needs to be optimized in order to obtain a continuous, homogeneous and uniform graphene layer(s) (Park, Meyer et al. 2010).

### 2.1.1.3 Beneficial effects of H<sub>2</sub>

If the growth conditions are properly adjusted, H<sub>2</sub> may be utilized to promote the synthesis and growth of graphene during CVD. H<sub>2</sub> in growth atmosphere influences the uniformity of graphene layers synthesized by CVD (Yu, Lian et al. 2008). With a high dosage of H<sub>2</sub> introduced 1 h before introducing the hydrocarbon gases, the uniformity of graphene is significantly enhanced, which suggests an annealing effect of H<sub>2</sub>. It is believed that H<sub>2</sub> can eliminate certain impurities (such as S and P) that may cause local variations in the carbon dissolvability in the metal substrates (Angermann and Hörz 1993). In addition, atomic H can remove defects in carbon (and anneal dangling bonds) at elevated temperatures.

### 2.1.2 Improvisations on CVD

In general, graphene synthesized by CVD has a high quality and a large area. Yet, they are multi-crystalline in structure (Li, Cai et al. 2009). This is attributable to multiple factors: the epitaxial growth mechanism of graphene on transition metal surfaces, the multi-crystalline nature of the catalyst substrate, and the simultaneous nucleation of C atoms from multiple sites of the substrate surface. Therefore, further scientific research is required for fabricating high quality graphene with large single crystal domains. The recent experimental observation clearly showed the domain formation of CVD synthesized graphene and the defects are lined along the boundaries of the domains (Li, Cai et al. 2009). There are many experimental studies on the growth mechanism of graphene on the catalyst surface (Loginova, Bartelt et al. 2008; Gruneis, Kummer et al. 2009; Loginova, Bartelt et al. 2009; McCarty, Feibelman et al. 2009; Starodub, Maier et al. 2009). McCarty and his co-workers (Loginova, Bartelt et al. 2008; Loginova, Bartelt et al. 2009; McCarty, Feibelman et al. 2009; Starodub, Maier et al. 2009) have highlighted the significance of C dimer super-saturation on the metal surface to initiate the nucleation of graphene. They have also shown that graphene nucleation preferentially occurs at metal steps rather than at terraces. While theoretical studies in this nucleation are still scarce, Chen and his co-workers have recently studied the formation of carbon monomer and dimer on transition metal terraces and steps to probe the epitaxial growth of graphene (Chen, Zhu et al. 2010).

The methods of graphene synthesis which preceded CVD are briefly mentioned below.

### 2.2 Exfoliation method

One of the earliest and simplest methods consisted in micromechanical exfoliation or cleavage of graphite (Novoselov, Geim et al. 2004; Novoselov, Geim et al. 2005; Novoselov, Jiang et al. 2005). Layer(s) of graphene are peeled off mechanically from highly ordered graphite using a Scotch tape and then deposited on a substrate e.g. SiO<sub>2</sub>. This is a simple yet efficient method, as graphene is obtained from highly ordered graphite crystals. Graphene extracted by microexfoliation shows very good electrical and structural quality. However, the shortcoming of this most elementary method is its non-scalability and production of uneven graphene films with small area.

### 2.3 Epitaxial growth

Graphene is also synthesizable by annealing of SiC crystal (Berger, Song et al. 2004; Berger, Song et al. 2006) at a very elevated temperature (~2000 K) in ultra-high vacuum. Thermal desorption of Si from the top layers of SiC crystalline wafer yields a multilayered graphene structure that behaves like graphene. The number of layers can be controlled by limiting time or temperature of the heating treatment. The quality and the number of layers in the samples depend on the SiC face used for their growth (Castro Neto, Guinea et al. 2009) (and references therein). Although the produced structure has a larger area than that obtainable by the exfoliation technique, still the coverage or area is way below the size required in electronic applications. Moreover, it is difficult to functionalize graphene obtained by this route.

### 2.4 Wet-chemistry approach

Wet-chemistry based approach is also employed to synthesize graphene by reduction of chemically synthesized graphene oxide (Stankovich, Dikin et al. 2007; Eda, Fanchini et al. 2008; Pichon 2008) (and references therein). Graphite is transformed into acid-intercalated graphite oxide by a severe oxidative treatment in sulphuric and nitric acid (Hummers and Offeman 1958). The intercalant is then rapidly evaporated at elevated temperatures, followed by its exposure to ultrasound or ball milling. Exfoliation of the graphite oxide readily occurs in aqueous medium due to the hydrophilicity of the former. Subsequent reduction of exfoliated graphite oxide sheets by hydrazine results in the precipitation of graphene owing to its hydrophobicity (Stankovich, Dikin et al. 2007). It is more versatile than the methods comprising exfoliation and epitaxial growth on SiC and easier to scale up. Yet, it has a poor control on the number of layers of graphene produced. Graphene synthesized by this method may remain partially oxidized, which potentially changes its electronic, optical, and mechanical properties.

## 3. Properties of graphene

The distinctive electronic, thermal and mechanical properties of graphene make it a very promising candidate for a wide range of applications in nanoscience and nanotechnology. The versatile properties of graphene are very well documented in the exponentially growing scientific literature. Some of its interesting properties and its technological implications are discussed hereafter.

### 3.1 Electronic properties

Graphene has immense potential for electronics for its extraordinarily high mobility of its charge carriers at room temperature. When Si-based technology is approaching its fundamental limits, graphene seems to be an ideal candidate to take over from silicon (Geim and Novoselov 2007). Yet, graphene is semi-metallic with no band gap, which severely limits its applications in electronics (Wei, Wang et al. 2010) due to its high leakage current in many applications. The electronic band gap plays a central role in modern device physics and technology and controls the performance of semiconductor devices. Moreover, it is a property inherent to semiconductors and insulators which considerably govern their transport and optical properties (Zhang, Tang et al. 2009). It has been possible to open and tune the band gap of graphene bilayers by applying an electric field (Zhang, Tang et al. 2009) or by doping (Ohta, Bostwick et al. 2006). These results have profound implications for

potential utilization of graphene in electronics. The structure of graphene can be tailored to change its electronic properties (spectrum) by several means discussed in the next sub-section. The structural manipulation may induce optical properties (i.e band-gap opening), which in turn gets incorporated into it, resulting in its potential for opto-electronic applications.

### 3.2 Optical properties

Quantum size effects show up when the  $\pi$  electrons in graphene are confined laterally e.g. in graphene segments (Zhang, Bertran et al. 1998; Feng, Lin et al. 2009) or graphene nanoribbons (GNR) (Han, Ouml et al. 2007). An energy gap opens up when carriers are confined to a quasi-one dimensional system like GNR. GNR shows optical properties which are sensitive to their width, family, crystallographic orientation and edge termination (Nakada, Fujita et al. 1996; Wakabayashi, Fujita et al. 1999); similar to the CNTs. The energy gap of lithographically patterned GNR structures has been found to scale inversely with the ribbon width, which demonstrates the possibility to engineer the band gap of graphene nanostructures by lithographic processes (Han, Ouml et al. 2007). An alternative route to induce the formation of a band gap is through the hydrogenation of graphene (Elias, Nair et al. 2009; Guisinger, Rutter et al. 2009; Samarakoon and Wang 2010). The modification of the carbon bonds associated with the hydrogenation preserves the crystalline order of the lattice but leads to rehybridization of the carbon atoms from a planar  $sp^2$  to a distorted  $sp^3$  state (Sofa, Chaudhari et al. 2007). Recent experimental studies have demonstrated reversible hydrogenation through heating (Elias, Nair et al. 2009). Our theoretical findings relevant to structure and size dependent PL in carbon nanostructures (Zhang, Bertran et al. 1998; Feng, Lin et al. 2009) are discussed in the following sub-section.

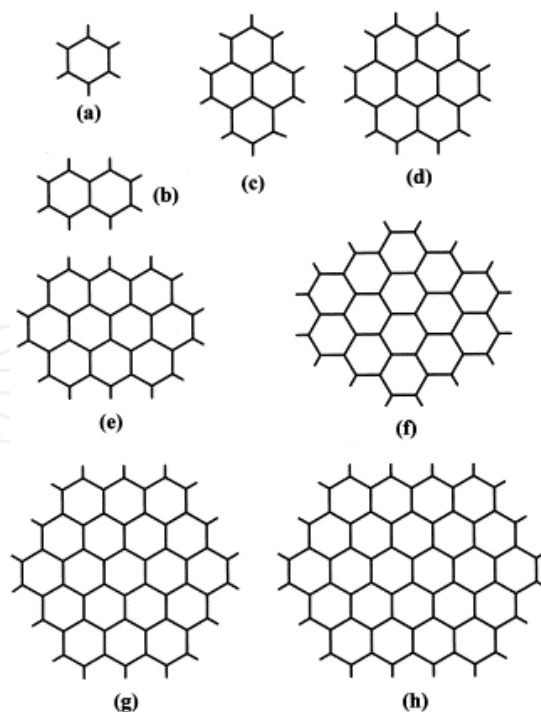


Fig. 2. Models for hexagonal clusters (or graphene segments): (a)  $C_6H_6$ , (b)  $C_{10}H_8$ , (c)  $C_{16}H_{10}$ , (d)  $C_{24}H_{12}$ , (e)  $C_{32}H_{14}$ , (f)  $C_{42}H_{16}$ , (g)  $C_{54}H_{18}$  and (h)  $C_{66}H_{18}$ . The terminated bonds indicate the sites of boundary hydrogen atoms (Zhang, Bertran et al. 1998).

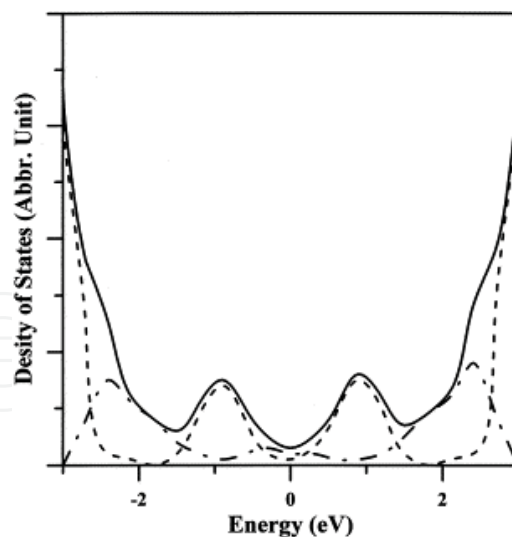


Fig. 3. Schematic diagram illustrates the distribution of band-gap states in a-C:H materials. A solid line indicates the total density of states (DOS); a dashed line represents the unlocalized states; and the dash-dotted line shows the localized states (Zhang, Bertran et al. 1998).

The broadband luminescence between 1.5 and 2.5 eV from carbon-based films has been attributed to the presence of a  $sp^2$  amorphous phase or graphite phase (Badzian, Badzian et al. 1988; Nemanich, Glass et al. 1988). The distribution of states within the energy gap introduced by an  $sp^2$  disordered phase in CVD diamond film has been considered as the origin of the broadband luminescence (Bergman, McClure et al. 1994), based on the theory of amorphous material (Street 1984). Further, the mechanism of luminescence and recombination in a-C:H and its alloys has been proposed (Robertson 1996 (a); Robertson 1996 (b); Silva, Robertson et al. 1996) to be due to a modification of the band edges in hydrogenated amorphous silicon. The band-tail states were assumed to arise from clusters of  $sp^2$  sites. The  $\pi$ -bonding  $sp^2$  phase has frequently been related to the origin of the luminescence (Rusli, Amaratunga et al. 1995; Bourée, Godet et al. 1996; Liu, Gangopadhyay et al. 1997). The broadband luminescence is commonly believed to be related to the gap/tail states produced from small  $sp^2$  clusters with various sizes and/or shapes. A new photoluminescence model taking account of individual cluster has presented a convincing mechanism (Demichelis, Schreiter et al. 1995). Still, clear pictures of which structures or shapes of  $sp^2$  carbon-clusters contribute to the highly efficient luminescence were missing. For a crystal diamond that is also a pure  $sp^3$ -bonded material, the gap is not only indirect but also wide (5.49 eV at 77 K (Collins 1993)). The gap of a nano-structural diamond-like crystallite may be even larger, and thus may not relate to the luminescence that is presently concerned in the range 1.5~2.5 eV generated by means of optical transition between band states. On the other hand, the  $\pi$ -bonding states of graphite lie closest to the Fermi level, so it does not seem realistic to relate the gap formed by these states to the luminescence between 1.5 and 2.5 eV, too. However, a nano-sized  $\pi$ -bonding  $sp^2$  cluster may show a fairly wide energy gap in comparison with that of the graphite material, as shown in our work (Zhang, Bertran et al. 1998), which coincides with the size-dependence rule that normally holds for many other materials. This feature has actually been seen in the calculations with a Hückel approximation for several  $sp^2$  carbon clusters (Robertson and O'Reilly 1987; Robertson 1995). However, the previous study was only qualitative and did not distinguish the

different features of states in the gap-tail caused by the individual  $sp^2$  carbon clusters due to their different sizes and/or shapes. Such a distinction, in our opinion, is very important for understanding the origin of highly efficient luminescence from carbon-based materials.

For the carbon-based materials described here, it is widely believed that both the size and shape determine the energy gap and the broadband luminescence (Demichelis, Schreiter et al. 1995; Robertson 1996 (a); Robertson 1996 (b); Silva, Robertson et al. 1996). However, any structural deviation from the stable configurations (for carbon, the stable structures are tetrahedral or  $sp^3$  and hexagonal or  $sp^2$ ) may produce localized states so that the energy gap is influenced. Obviously, the localized states do not relate to the efficient, room temperature luminescence. Thus, the small clusters with structures such as a fivefold ring, sevenfold ring and off-plane hexagonal that are not the stable hexagonal structures are doubtful for the main contribution to the efficient broadband luminescence. Also, the main source for such luminescence would be the stable hexagonal carbon clusters. We carried out calculations for a series of tetrahedral and hexagonal atomic clusters, shown in Fig 2 based on semi-empirical molecular orbital and density functional theories to determine the size-dependence effect of the energy gap in such clusters. We have classified the band-tail states into localized and confined, as shown in Fig 3 in order to emphasize the role of hexagonal planar shape of carbon-clusters in the broad band visible PL. The localized states result from the structural deviation from graphite-like configuration, and the associated luminescence may be described by using the conventional theory for amorphous materials. The confined states are generated due to the existence of stable graphite-like local structures with various sizes shown in Fig. 2 and are the main factor for giving efficient, room-temperature luminescence. Our calculations of a series of small hexagonal carbon clusters shown in Fig. 2 demonstrate that the energy-gap distribution, due to the difference in size, is considerably broad, which explains the broadband feature of luminescence. Weak  $\pi$ - $\pi$  interaction enables multilayer stacking of graphene sheets in different possible ways shown in Fig 4 (Feng, Lin et al. 2009) and thereby helps the formation and stability of large-sized  $sp^2$  C-H films. Our calculations show that the energy gaps of graphene are strongly dependent on their sizes (Feng, Lin et al. 2009), while the stacking order and the number of stacked layers have a minor influence. The energy gap is found to decrease with the increasing size, as shown in Fig 5. It turns out that by controlling the formation of graphene during CVD, it would be possible to control the size of the growing graphene and thereby tune its luminescent properties by utilizing our results on the size dependence of energy gap.

### 3.3 Non-covalent binding properties

The weak, intermolecular, vdW,  $\pi$ - $\pi$  interactions (Hunter and Sanders 1990) play a crucial role in the crystal packing of organic molecules containing aromatic rings (Desiraju and Gavezzotti 1989; Hunter, Lawson et al. 2001), the intercalation of certain drug molecules into DNA (Brana, Cacho et al. 2001), the binding affinities of host-guest complexes (Muehldorf, Van Engen et al. 1988; Ferguson, Sanford et al. 1991; Chipot, Jaffe et al. 1996), as well as the three-dimensional structures of biological systems, including proteins and nucleic acids, and their molecular organization and recognition processes (Burley and Petsko 1985; Blundell, Singh et al. 1986; Hobza, Selzle et al. 1994). Graphene sheets can be stacked into bilayers and multilayers by virtue of  $\pi$ - $\pi$  interactions between the neighboring sheets. The electronic properties of graphene multilayers vary with the stacking order, and rapidly evolve with the number of layers, approaching the 3D limit of graphite (Geim and Novoselov 2007; Castro Neto, Guinea et al. 2009).

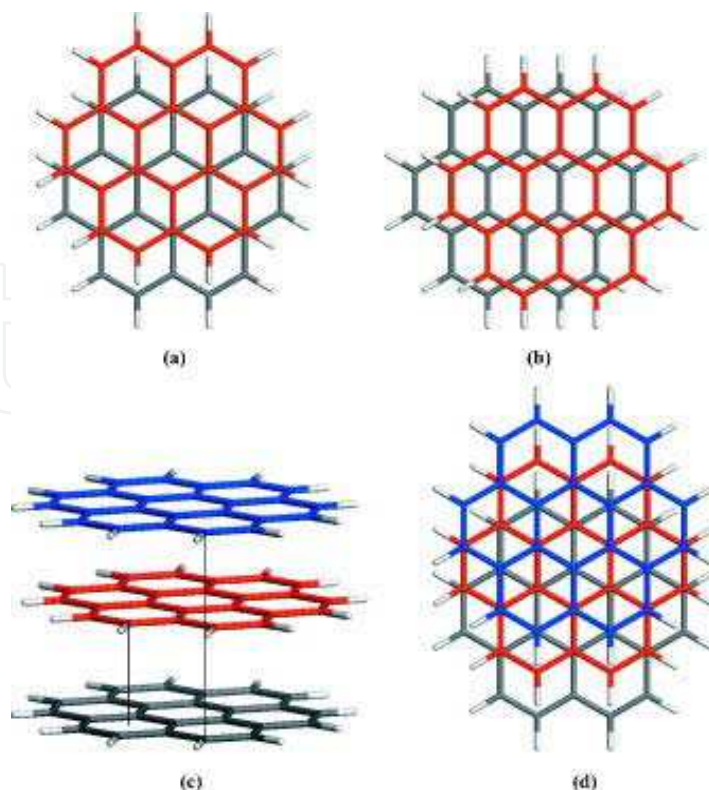


Fig. 4. Top views of the arrangement of the carbon atoms in two adjacent coronene planes in (a) staggered and (b) parallel-displaced stacking, and in coronene trimers with (c) ABA and (d) ABC stacking; gray, red, and blue represent the lowest, middle, and top layers, respectively (Feng, Lin et al. 2009).

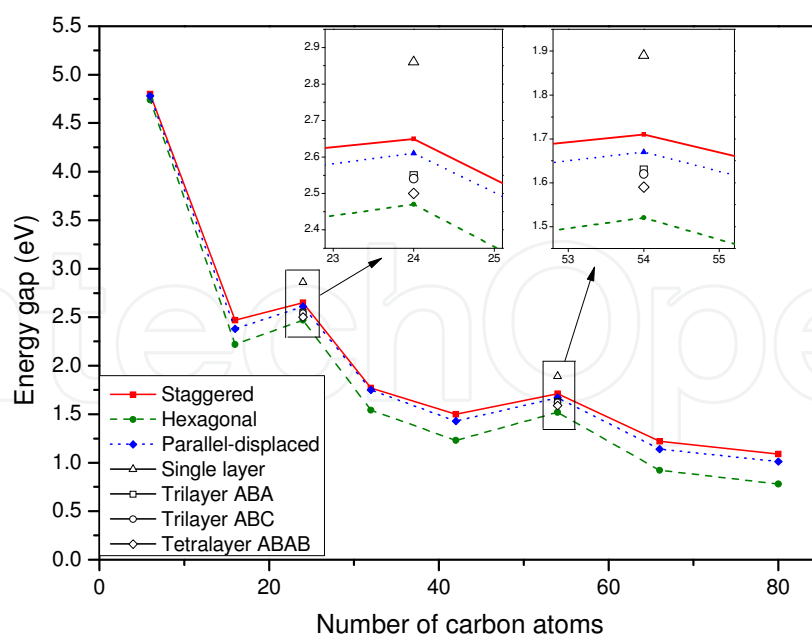


Fig. 5. Variation of the energy gap with the size of graphene sheet model dimers for the staggered, hexagonal, and parallel-displaced stackings, respectively. The open symbols and the insets show the energy gaps of  $C_{24}H_{12}$  and  $C_{54}H_{18}$  monomers, and their trimers with ABA and ABC stackings, and tetramers with an ABAB sequence (Feng, Lin et al. 2009).

Theoretically, it is challenging to model weak vdW interaction with the conventional DFT unless an appropriate, correction term for vdW interaction is incorporated. With such a treatment, we have shown in our work that the stacked graphene segments can be held together in different orientations by  $\pi$ - $\pi$  interactions and the binding energy is strongly dependent on the size of the PAH, on stacking order, and on the number of stacked layers (Feng, Lin et al. 2009). A graphene bilayer has very unusual electronic properties, such as the anomalous integer quantum Hall effect that significantly changes with respect to a single layer (McCann and Fal'ko 2006; Novoselov, McCann et al. 2006; Malard, Nilsson et al. 2007), and which can be used to distinguish between a graphene bilayer and a monolayer. Moreover, as already mentioned in a preceding sub-section, the band-gap of graphene bilayer is tunable in different ways (Ohta, Bostwick et al. 2006; Zhang, Tang et al. 2009). The importance of graphene bilayers emphasizes the need to understand the binding between the two sheets in graphene bilayers. We have shown in our work using dimer, bilayer models that the binding energy increases with size until it saturates when it reaches the size of about 80 atoms (Feng, Lin et al. 2009). A clear understanding of the weak vdW interactions discussed in the section is relevant to some potential applications of graphene.

## 4. Physisorption and related applications

### 4.1 Water physisorption and novel ice structure formation

A water cluster adsorbed on a graphite surface is a prototypical weakly bound vdW  $\pi$ -system that involves water-graphite and water-water interactions. Our investigations show that the binding energy of water clusters interacting with graphite is dependent on the number of water molecules that form hydrogen bonds, but is independent of the water cluster size. Furthermore, we have found that these physically adsorbed or physisorbed water clusters show little change in their IR peak position and leave an almost perfect planar graphite surface (Lin, Zhang et al. 2005). SW-CNTs provide a well-defined nanoscale cylindrical pore that can serve as a nanometer-sized capillary in the fabrication of quasi-one-dimensional (Q1D) materials by filling SW-CNTs with chosen materials (Saito, Dresselhaus et al. 1998; Ugarte, Stoeckli et al. 1998). Even though water has been extensively studied, some of its properties remain partially unknown. A significant number of them are related to the behavior of water under confinement within nanoscale Q1D channels such as SW-CNTs, and the confined water is expected to exhibit different physical properties from its bulk counterparts. Since many similar scientifically relevant systems can be found in nature, this issue is of great interest to biology, geology, and materials science (Sansom and Biggin 2001).

We have systematically studied using a self-consistent charge density-functional tight-binding method complemented with an empirical vdW force correction to show that water molecules can form cylindrical crystalline structures (see Fig 6), referred to as INTs, by hydrogen bonding under confinement within single-walled carbon nanotubes (Feng, Zhang et al. 2007). Each water molecule in the optimized INTs is hydrogen bonded to its four nearest-neighbor water molecules in a tetra-coordinate configuration, and all water molecules constituted a novel cylindrical ice phase with ordered hydrogen-bond network, which is weaker than that of conventional hexagonal ice.

Our calculations show that for the confining CNTs, e.g., (16,0) SW-CNT, the HOMO-LUMO gap was slightly reduced from 0.567 to 0.554 eV while the Fermi level increased from -4.619 to -4.607 eV after it was filled with 6-gonal INT. Figure 7 also shows that both the HOMO and LUMO of INT-CNT complex are solely composed of the ones of the confining CNT and

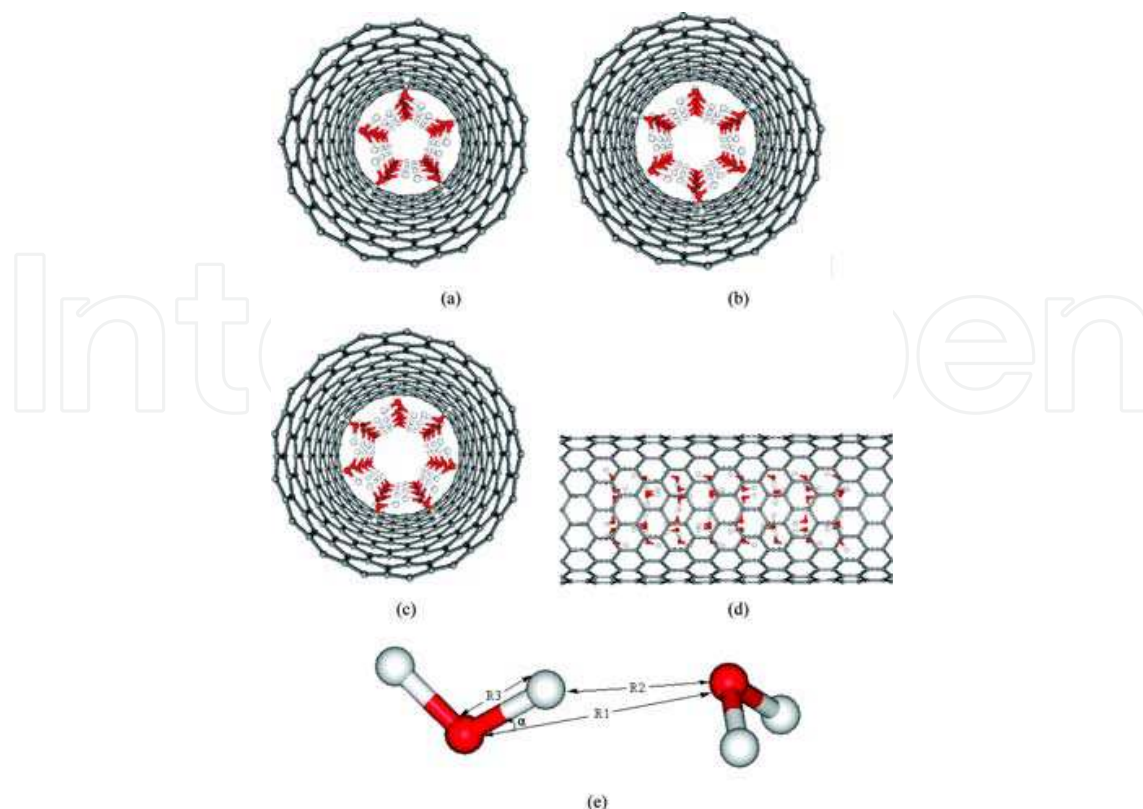


Fig. 6. Optimized (a) pentagonal, (b) hexagonal, and (c) heptagonal INT confined in zigzag ( $l,0$ ) SW-CNT,  $l = 15, 16$ , and  $17$ , respectively, and (d) side view of hexagonal INT model; (e) structural parameters used for quantifying hydrogen bond as discussed in the text. Red, white, and gray spheres represent oxygen, hydrogen, and carbon atoms, respectively (Feng, Zhang et al. 2007).

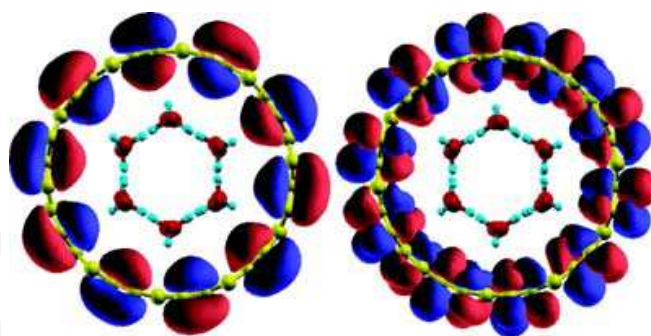


Fig. 7. Two isosurfaces of the wave functions of the HOMO (left) and LUMO (right) derived from bands at the  $\Gamma$  point for the 6-gonal INT confined in the zigzag ( $16,0$ ) SW-CNT (Feng, Zhang et al. 2007).

that there is no overlap between molecular orbitals from CNT and INT. Consequently, it can be derived that water molecules of INTs can hardly interact with confining CNTs via the ordinary OH/ $\pi$  interactions, which are the main intermolecular forces between the water molecule and aromatic rings, for instance, in water-benzene/graphite complexes (Lin, Zhang et al. 2005). The reason is that each water molecule of INTs is hydrogen bonded to two water molecules with its two O-H bonds as hydrogen donors, and there is no other O-H bond available for a water molecule to interact with the hexagonal carbon rings of

confining CNTs via OH/ $\pi$  interaction. We have revealed that the unique crystalline structures of INTs are mainly due to the steric hindrance effect induced by the confining CNT rather than the ordinary OH/ $\pi$  interaction between INT and CNT.

## 4.2 Hydrogen molecule physisorption and storage

Hydrogen physisorption by carbon-based nanostructures, which has potential for hydrogen storage, still remains challenging. The current preparative methods for CNTs generate heterogeneous tubes varying in length, diameter, and chirality. The presence of multiply ( $n$ ,  $m$ ) chiral SW-CNTs in a given sample poses a major barrier towards realizing many potential applications of CNTs. It may also contribute to the many inconsistencies in the experimental results.

The interaction between H<sub>2</sub> and CNT is a typical  $\pi$ -involved weak interaction. Using an approximate density functional method augmented with a vdW dispersion term, we have systematically investigated the role of CNT's curvature and chirality on the physisorption of H<sub>2</sub>. In our work, we have explored the different possible physisorption sites for H<sub>2</sub> molecule on SW-CNT, as shown in Fig 8. Based on our results shown in Fig 9, we propose that CNTs with diameter of 6–7 Å, such as (5, 5), (8, 0), and (6, 3) tubes, are energetically optimal candidates for physisorption of H<sub>2</sub>. In this relatively narrow range of diameters, the internal adsorption binding energies are around –0.22 eV, which is three times as large as that of H<sub>2</sub> on graphene surface; for external adsorption, the binding energy of –0.061 eV is just 18% below that of H<sub>2</sub> on graphene surface. It is conceivable that the inconsistencies in the experimental results (in terms of the hydrogen storage capacities of CNTs) were caused in part by the varying diameters of the as-prepared CNT samples used. We have found that nanotube's curvature plays an important role in the physisorption process of hydrogen, while the chirality of the tube has a negligible effect.

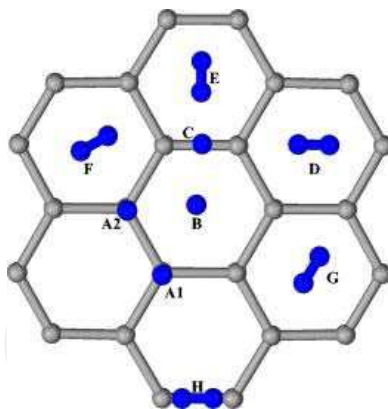


Fig. 8. Different adsorption sites for a hydrogen molecule on a segment of armchair SW-CNTs (Fan, Zhang et al. 2009).

## 4.3 Interaction with bio molecules, its relevance to biosensing

### 4.3.1 Flavin Adenine dinucleotide (FAD)

FAD is in the redox active group of flavoenzymes that catalyzes important biological redox reactions and is perhaps the most versatile of all of the redox coenzymes. We simulated the adsorption procedure of the FAD on the semiconducting (10,0) and the metallic (5,5) carbon nanotubes (CNTs) using a density functional tight binding method with the inclusion of an empirical dispersion term in total energy.

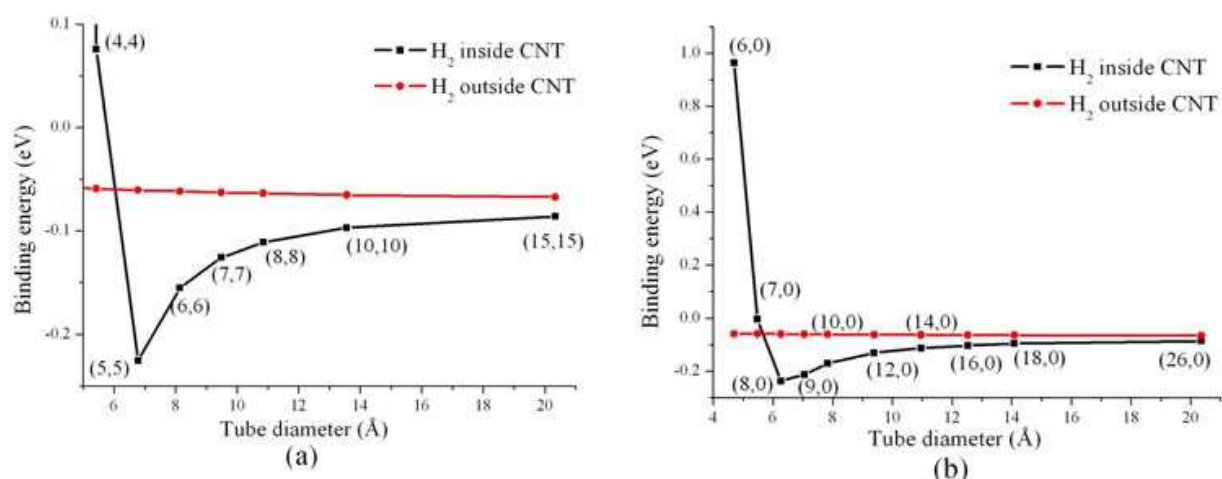


Fig. 9. Optimized binding energies of molecular hydrogen internally and externally adsorbed to CNTs for armchair (a) and zigzag (b) CNTs (Fan, Zhang et al. 2009).

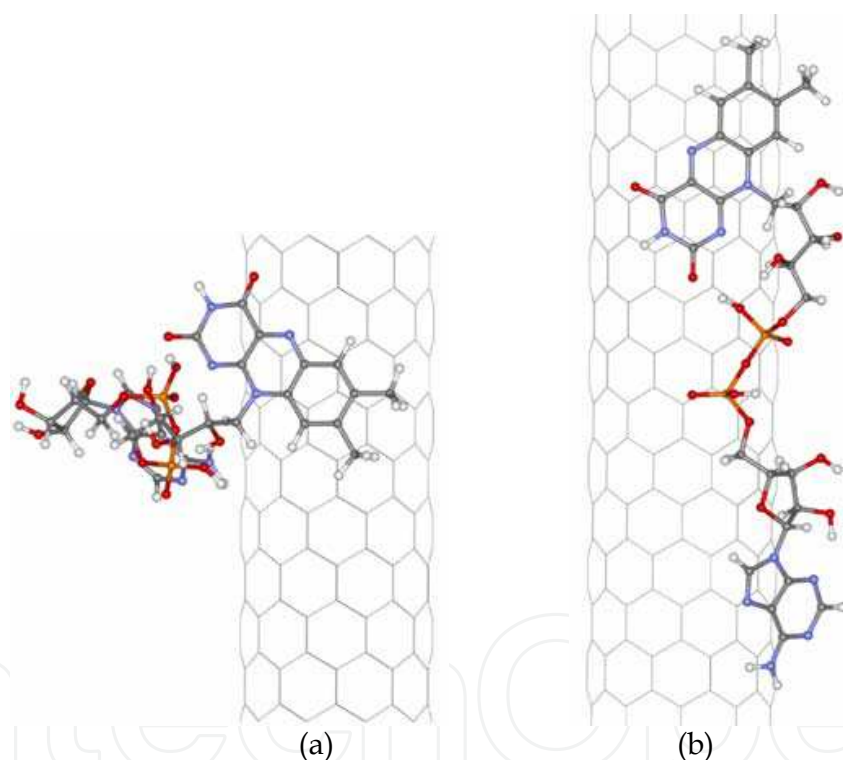


Fig. 10. Optimized structures of the (a) perpendicular and (b) parallel configurations of FAD adsorbed on (10,0) CNT (Lin, Zhang et al. 2007).

The flavin and adenine groups of FAD could be attracted to the CNT surface through  $\pi$ - $\pi$  stacking but remain at the physisorption distances. The configurations with the FAD long axis perpendicular or parallel to the tube axes of the semiconducting (10,0) and metallic (5,5) CNTs, shown in Fig 10 were almost energetically degenerate. In the FAD/(10,0) system, the FAD flavin group contributed more components in the band structure at the Fermi energy level (see Fig 11), which was responsible for the enhancement of the electronic transferability as observed in a cyclic voltammogram experiment (Guisseppi-Elie, Lei et al. 2002).

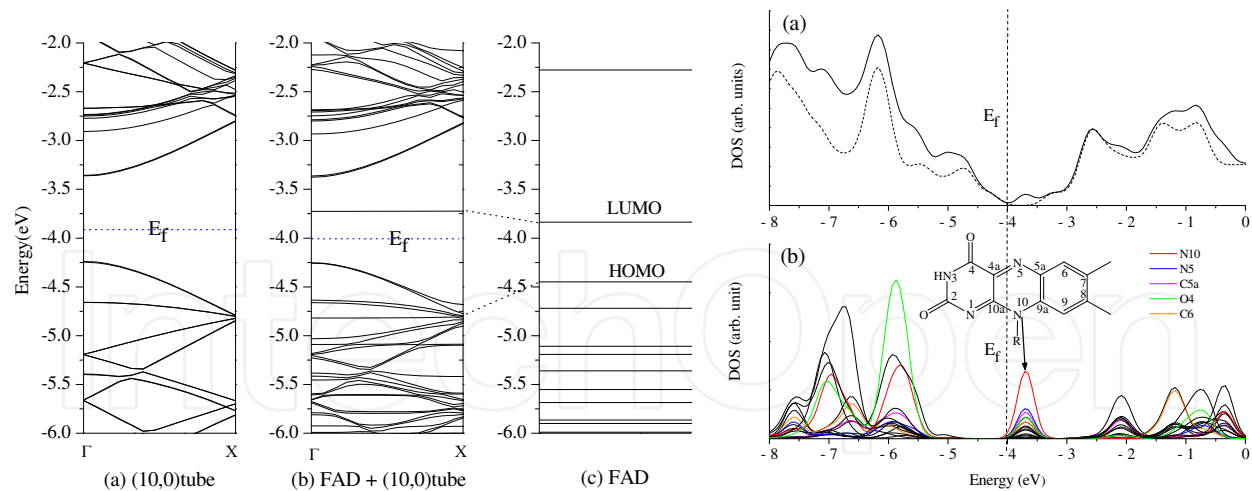


Fig. 11. (Left) Band structure of (a) an isolated (10,0) CNT, (b) FAD/(10,0), and (c) an isolated FAD molecule calculated with the same periodic condition. (Right) Total density of states of (10,0) CNT (dashed line) and FAD/(10,0) (solid line), and (b) projected density of states of O, N, and C atoms of the FAD flavin group in the FAD/(10,0) system. The largest five components were marked with different colors, and those from others atoms are shown as black color (Lin, Zhang et al. 2007).

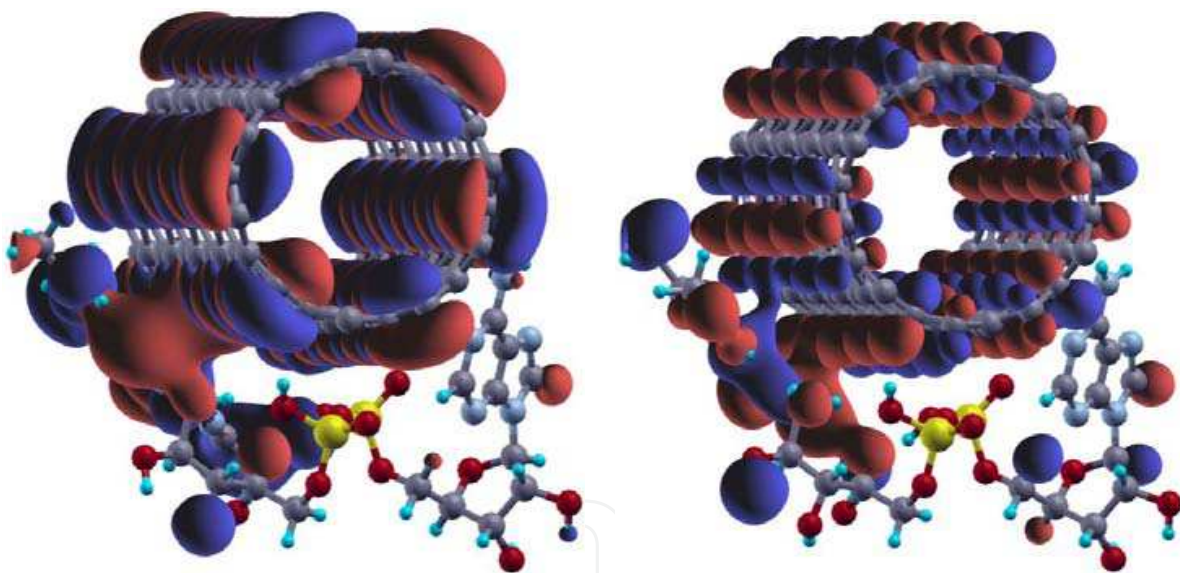


Fig. 12. Isosurfaces of the wave functions of the HOMO (left panel) and LUMO (right panel) derived bands at the  $\Gamma$  point for the FAD adsorbed on the (10,0) CNT surface. The isovalue is 0.02 au (Lin, Zhang et al. 2007).

The total DOS and projected density of states (PDOS) of FAD/(10,0) showed that the flavin group contributed significant components at the Fermi energy while the adenine group had few such components and the phosphate group had none. Hence, the flavin group served as the active unit relating to the electronic mobility of the FAD interacting with the CNT. In the FAD/(10,0) system, both HOMO and LUMO have significant contribution from the FAD flavin group (Fig. 12). The HOMO and LUMO of the FAD/(5,5) system showed their main features contributed by the CNT and the FAD flavin group respectively. This shows that the CNT may have contributed to the electron excitation procedure.

Despite a physisorption, there was a noticeable effect on the CNT electronic structure and mobility. Our results have prompted others (Ju, Doll et al. 2008; Ju and Papadimitrakopoulos 2008; Ju, Kopcha et al. 2009) to experimentally explore the properties of CNTs functionalized by flavin mononucleotide and its analogue.

#### 4.3.2 Peptides

SW-CNTs have potential for biological applications ranging from biomedical sensors to drug delivery (Martin and Kohli 2003; Li, Ng et al. 2005; Contarino, Sergi et al. 2006). Yet, such biological applications have, so far, been limited due to two major obstacles: hydrophobicity and conformational heterogeneity. Although the solubility in water can be improved by chemically modifying the SW-CNTs through covalent bonding of various functional groups to the nanotubes (Hirsch 2002; Huang, Fernando et al. 2003), these modifications can perturb the intrinsic properties of SW-CNTs, such as electrical properties. As a result, alternative approaches using the non-covalent adsorption of surfactants (O'Connell, Bachilo et al. 2002), polymers (Dalton, Blau et al. 2001) and biomolecules (Zheng, Jagota et al. 2003; Zheng, Jagota et al. 2003; Numata, Asai et al. 2005) to solubilize the SW-CNTs have been proposed and tested. To that end, much research attention has been focused on the design and utilization of polypeptide/CNT complexes because of their functionality in biological systems (Dieckmann, Dalton et al. 2003; Zorbas, Ortiz-Acevedo et al. 2004; Ortiz-Acevedo, Xie et al. 2005; Pender, Sowards et al. 2005; Karajanagi, Yang et al. 2006; Su, Leung et al. 2006) recently.

We investigated the binding nature of three peptides (inactive NB1 and active B1 and B3) to single-walled carbon nanotubes (SWCNTs) using a density functional tight-binding (DFTB) method with an empirical vdW force correction (Fan, Zeng et al. 2009). Figure 13 shows the optimized geometries of the three peptides/(5,5) CNT complexes. We have shown that peptides (inactive NB1 and active B1 and B3) could be spontaneously attracted to the sidewall of CNTs through  $\pi$ - $\pi$  and/or H- $\pi$  stacking, which is at the physisorption distance. The competition of  $\pi$ - $\pi$  and/or H- $\pi$  stacking plays a key role in binding the peptides to the CNTs, thus, determining and stabilizing the binding of the peptide/CNT systems. The preservation of the helical conformation upon peptide B3 adsorption to the side wall of SWCNT is consistent with the experimental observation obtained using CD spectroscopy (Su, Leung et al. 2006). Our results demonstrate that the geometric structure of CNT remains almost unchanged after the adsorption of peptides. Moreover, the isosurfaces of the selected frontier orbitals show that the  $\pi$ -electronic structures of the CNTs are preserved upon the non-covalent adsorption of B3 peptides, which is similar to the features for simple planar organic molecules adsorbed on CNTs (Tournus and Charlier 2005; Tournus, Latil et al. 2005). DOS in Fig 14 furthers our understanding of its electronic properties. Compared with the pristine semiconducting (8,0) CNT, the DOS of the B3/(8,0) CNT shows new states near the Fermi level, which were contributed by the peptide B3. Still, the nature of physisorption is shown since the total DOS preserves the features of the DOS of pristine (8,0) CNT.

We find new DOS, composed mainly of the HOMO of B3 molecular orbitals, between the (8,0) CNT conduction and valence bands. Hence, the band gap of the system has sharply decreased from the pristine (8,0) tube 0.58 to 0.29 eV of the complexes. Similar finding of band gap reduction has been found in the (7,3) polyC-DNA complex compared to the free semiconducting (7,3) tube (Enyashin and et al. 2007). The finding of the new DOS formed between the (8,0) CNT conduction and valence bands is quite similar to our previous study of FAD/(10,0) CNT (Lin, Zhang et al. 2007). This implies that the non-covalent modification

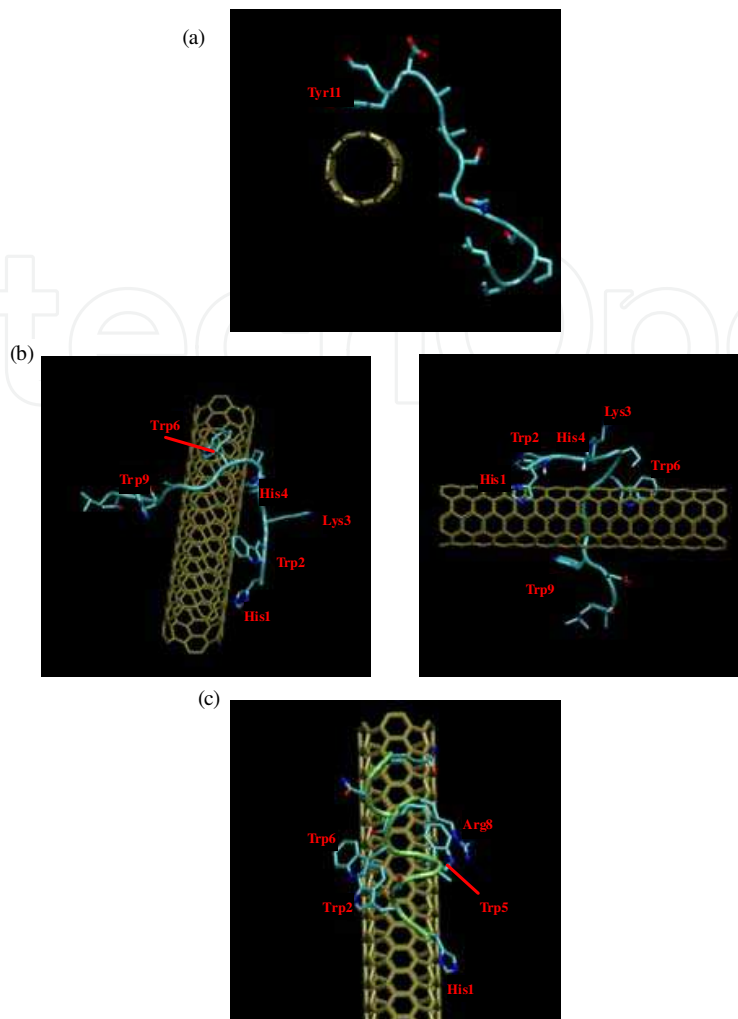


Fig. 13. Illustration of the peptide/(5,5) CNT interactions: (a) inactive peptide NB1, (b) the active peptide B1, and (c) the active peptide B3. The  $\pi$ - $\pi$  stacking and XH- $\pi$  (X = C and N) interactions are displayed in the left and right panels for the (b) B1/CNT complex, respectively. Key residues are labelled in red (Fan, Zeng et al. 2009).

of SW-CNTs by the active peptides might increase the former's electron transfer capabilities. Our study confirms the experimental findings (Wang, Humphreys et al. 2003) on the key role of the arene parts, such as His and Trp, and also agree with earlier theoretical reports (Chen, Hong et al. 2006; Tomásio and Walsh 2007).

## 5. Conclusion

A proper understanding of the growth and properties of graphene is a must for its optimal utilization. We have clarified the functionality of H in etching out the  $sp^2$  phase of carbon nanostructures and thereby in promoting the  $sp^3$  phase during CVD growth of graphene/diamond. The growth atmosphere and conditions needs to be properly adjusted during CVD growth in order to avoid this etching effect of hydrogen and invoke the beneficial effects of  $H_2$ . The size of graphene segments needs to be controlled during its growth by CVD in order to tune its luminescent properties as the energy gap scales inversely with the size of graphene segments. The structure of PAHs or graphene segments,

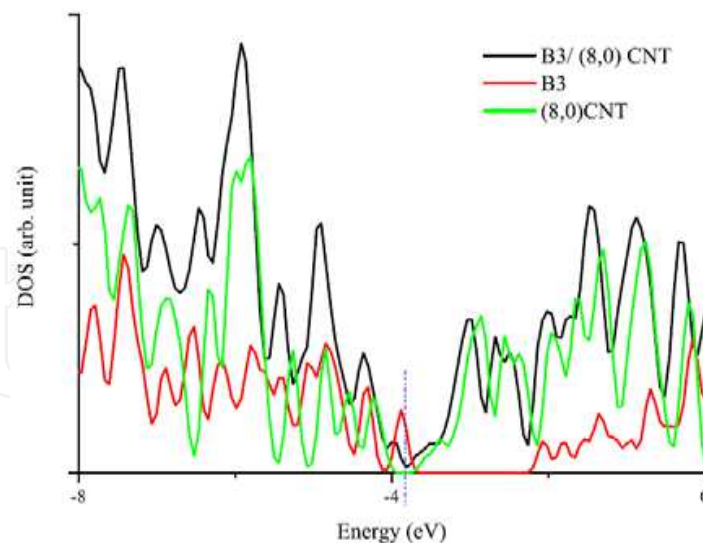


Fig. 14. Total density of states for B3/(8,0) CNT (Fan, Zeng et al. 2009).

both mono and multi layered, is solely attributed to visible and efficient luminescence at room temperature in our comprehensive findings. Weak, intermolecular, vdW interactions and its importance have been thoroughly explored in our work. We have found the  $\pi$ - $\pi$  weak vdW interaction to bind together the planar graphene segments or PAHs in bilayers and multi-layers over a large size range. Besides, in our theoretical studies, the weak interactions of graphene with some important bio molecules provide crucial clues to its possible bio applications. For instance, the encapsulation of water molecules within hydrophobic CNTs provides pointers to the capillary functionality of biological nanopores. We have practically ruled out the role of chirality of CNTs in binding  $H_2$  molecules, while we have pointed out the role of curvature of CNTs in the same. This has important implications for the hydrogen storage potential of CNTs. Furthermore, we have highlighted the importance of weak interaction of CNTs with a few important biomolecules in preserving the chemical, electrical and other properties of the former. The weak interaction was found to enhance the electron transfer capabilities of some bio molecules in our study. This signifies the bio-compatibility of CNTs and its viability in different bio and other practical applications. A good understanding of the binding or interaction between biomolecules and CNTs obtained from our work provides useful indicators for designing biosensors and drug delivery devices with bio-functionalized CNTs.

## 6. References

- Angermann, H. H. and G. Hörz (1993). Influence of sulfur on surface carbon monolayer formation and graphite growth on nickel. *Applied Surface Science*,70-71,Part 1,(June 02, 1993) (163-168),0169-4332
- Badzian, A. R., T. Badzian, et al. (1988). Crystallization of diamond crystals and films by microwave assisted CVD (Part II). *Materials Research Bulletin*,23,4,(April, 1988) (531-548),0025-5408
- Barone, V., O. Hod, et al. (2006). Electronic Structure and Stability of Semiconducting Graphene Nanoribbons. *Nano Letters*,6,12,(November 24, 2006) (2748-2754),1530-6984

- Berger, C., Z. Song, et al. (2004). Ultrathin Epitaxial Graphite: 2D Electron Gas Properties and a Route toward Graphene-based Nanoelectronics. *Journal of Physical Chemistry B*,108,52,(December 3, 2004) (19912-19916),1520-6106
- Berger, C., Z. Song, et al. (2006). Electronic Confinement and Coherence in Patterned Epitaxial Graphene. *Science*,312,5777,(May 26, 2006) (1191-1196), 0036-8075
- Bergman, L., M. T. McClure, et al. (1994). The origin of the broadband luminescence and the effect of nitrogen doping on the optical properties of diamond films. *Journal of Applied Physics*,76,5,(May 23, 1994) (3020-3027),0021-8979
- Blundell, T., J. Singh, et al. (1986). Aromatic Interactions. *Science*,234,4779,(November 21, 1986) (1005-1005),0036-8075
- Bourée, J. E., C. Godet, et al. (1996). Optical and luminescence properties of polymer-like a-C:H films deposited in a dual-mode PECVD reactor. *Journal of Non-Crystalline Solids*,198-200,Part 2,(May 02,1996) (623-627),0022-3093
- Brana, M. F., M. Cacho, et al. (2001). Intercalators as anticancer drugs. *Current Pharmaceutical Design*,7,17,(November, 2001) (1745-1780),1381-6128
- Burley, S. and G. Petsko (1985). Aromatic-aromatic interaction: a mechanism of protein structure stabilization. *Science*,229,4708,(July 5, 1985) (23-28),0036-8075
- Castro Neto, A. H., F. Guinea, et al. (2009). The electronic properties of graphene. *Reviews of Modern Physics*,81,1,(January 14, 2009) (109-162),0034-6861
- Chen, H., W. Zhu, et al. (2010). Contrasting behavior of carbon nucleation in the initial stages of graphene epitaxial growth on stepped metal surfaces. *Physical Review Letters*,104,18,(May 7, 2010) (186101-186104),0031-9007
- Chen, Q., Y. Hong, et al. (2006). Chaotic behaviors and toroidal/spherical attractors generated by discontinuous dynamics. *Physica A: Statistical and Theoretical Physics*,371,2,(November 15, 2006) (293-302),0378-4371
- Chipot, C., R. Jaffe, et al. (1996). Benzene Dimer: A Good Model for  $\pi$ - $\pi$  Interactions in Proteins? A Comparison between the Benzene and the Toluene Dimers in the Gas Phase and in an Aqueous Solution. *Journal of the American Chemical Society*,118,45,(November 13, 1996) (11217-11224),0002-7863
- Collins, A. T. (1993). Intrinsic and extrinsic absorption and luminescence in diamond. *Physica B: Physics of Condensed Matter*,185,1-4,(April, 1993) (284-296)
- Contarino, M. R., M. Sergi, et al. (2006). Modular, self-assembling peptide linkers for stable and regenerable carbon nanotube biosensor interfaces. *Journal of Molecular Recognition*,19,4,(July/August, 2006) (363-371),1099-1352
- Dalton, A. B., W. J. Blau, et al. (2001). A functional conjugated polymer to process, purify and selectively interact with single wall carbon nanotubes. *Synthetic Metals*,121,1-3,(March 15, 2001) (1217-1218),0379-6779
- Davis, J. W., A. A. Haasz, et al. (1987). Flux and energy dependence of methane production from graphite due to H<sup>+</sup> impact. *Journal of Nuclear Materials*,145-147,(February 2, 1987) (417-420),0022-3115
- Demichelis, F., S. Schreiter, et al. (1995). Photoluminescence in a-C:H films. *Physical Review B*,51,4,(January 15, 1995) (2143-2147),1050-2947
- Desiraju, G. R. and A. Gavezzotti (1989). From molecular to crystal structure; polynuclear aromatic hydrocarbons. *Journal of the Chemical Society, Chemical Communications*10, (621-623),0022-4936

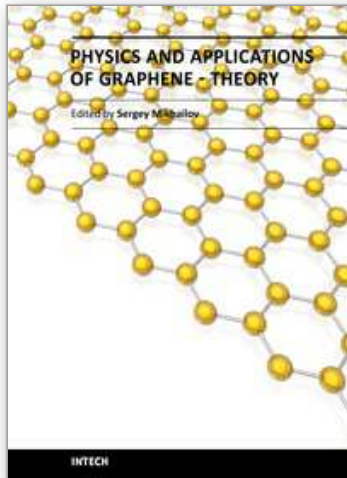
- Dieckmann, G. R., A. B. Dalton, et al. (2003). Controlled Assembly of Carbon Nanotubes by Designed Amphiphilic Peptide Helices. *Journal of the American Chemical Society*,125,7,(February 19, 2003) (1770-1777),0002-7863
- Donnelly, C. M., R. W. McCullough, et al. (1997). Etching of graphite and diamond by thermal energy hydrogen atoms. *Diamond and Related Materials*,6,5-7,(April, 1997) (787-790),0925-9635
- Eda, G., G. Fanchini, et al. (2008). Large-area ultrathin films of reduced graphene oxide as a transparent and flexible electronic material. *Nature Nanotechnology* 3,5,(April 6, 2008) (270-274),1748-3387
- Elias, D. C., R. R. Nair, et al. (2009). Control of Graphene's Properties by Reversible Hydrogenation: Evidence for Graphane. *Science*,323,5914,(January 30, 2009) (610-613),0036-8075
- Enyashin, A. N. and et al. (2007). DNA-wrapped carbon nanotubes. *Nanotechnology*,18,24,(May 25, 2007) (245702-245710),0957-4484
- Fan, W. J., J. Zeng, et al. (2009). Quantum Mechanical Quantification of Weakly Interacting Complexes of Peptides with Single-Walled Carbon Nanotubes. *Journal of Chemical Theory and Computation*,5,10,(October, 2009) (2879-2885),1549-9618
- Fan, W. J., R. Q. Zhang, et al. (2009). Prediction of energetically optimal single-walled carbon nanotubes for hydrogen physisorption. *Applied Physics Letters*,95,1,(July 10, 2009) (013116-013113),0003-6951
- Fang, R. c. (1991). Emission properties of amorphous silicon and carbon films. *Journal of Luminescence*,48-49,Part 2,(January-February, 1991) (IN5-IN6),0022-2313
- Feng, C., C. S. Lin, et al. (2009). Stacking of polycyclic aromatic hydrocarbons as prototype for graphene multilayers, studied using density functional theory augmented with a dispersion term. *The Journal of Chemical Physics*,131,19,(November 16, 2009) (194702-194708)
- Feng, C., C. S. Lin, et al. (2010). pi-pi INTERACTION IN BENZENE DIMER STUDIED USING DENSITY FUNCTIONAL THEORY AUGMENTED WITH AN EMPIRICAL DISPERSION TERM. *Journal of Theoretical & Computational Chemistry*,9,(June 2, 2009) (109-123),0219-6336
- Feng, C., R. Q. Zhang, et al. (2007). Signatures in Vibrational Spectra of Ice Nanotubes Revealed by a Density Functional Tight Binding Method. *The Journal of Physical Chemistry C*,111,38,(July 20, 2007) (14131-14138),1932-7447
- Ferguson, S. B., E. M. Sanford, et al. (1991). Cyclophane-arene inclusion complexation in protic solvents: solvent effects versus electron donor-acceptor interactions. *Journal of the American Chemical Society*,113,14,(July, 1991) (5410-5419),0002-7863
- Fukui, K. and H. Fujimoto (1997). *Frontier Orbitals and Reaction Paths: Selected Papers of Kenichi Fukui*,World Scientific: Singapore River Edge, NJ
- Gapozzi, V., G. Casamassima, et al. (1996). *Solid State Communications*,98, (853)
- Geim, A. K. and K. S. Novoselov (2007). The rise of graphene. *Nat Mater*,6,3, (183-191),1476-1122
- Gruneis, A., K. Kummer, et al. (2009). *New J. Phys.*,11, (9)
- Guiseppe-Elie, A., C. H. Lei, et al. (2002). *Nanotechnology*,13,, (559),
- Guisinger, N. P., G. M. Rutter, et al. (2009). Exposure of Epitaxial Graphene on SiC(0001) to Atomic Hydrogen. *Nano Letters*,9,4, (1462-1466),1530-6984

- Haluska, M., M. Hirscher, et al. (2004). Interaction of hydrogen isotopes with carbon nanostructures. *Materials Science and Engineering B: Solid-State Materials for Advanced Technology*,108,1-2, (130-133)
- Han, M. Y., Ouml, et al. (2007). Energy Band-Gap Engineering of Graphene Nanoribbons. *Physical Review Letters*,98,20, (206805)
- Harris, S. J., G. L. Doll, et al. (1995). *Appl. Phys. Lett.*,67,, (2314),
- Hirsch, A. (2002). Functionalization of Single-Walled Carbon Nanotubes. *Angewandte Chemie International Edition*,41,11, (1853-1859),1521-3773
- Hobza, P., H. L. Selzle, et al. (1994). Structure and Properties of Benzene-Containing Molecular Clusters: Nonempirical ab Initio Calculations and Experiments. *Chemical Reviews*,94,7, (1767-1785),0009-2665
- Hoffmann, R. (1988). *Rev. Mod. Phys.*,60,, (601),
- Huang, W., S. Fernando, et al. (2003). Preferential Solubilization of Smaller Single-Walled Carbon Nanotubes in Sequential Functionalization Reactions. *Langmuir*,19,17, (7084-7088),0743-7463
- Hummer, G., J. C. Rasaiah, et al. (2001). Water conduction through the hydrophobic channel of a carbon nanotube. *Nature*,414,6860, (188-190),0028-0836
- Hummers, W. S. and R. E. Offeman (1958). Preparation of Graphitic Oxide. *Journal of the American Chemical Society*,80,6, (1339-1339),0002-7863
- Hunter, C. A., K. R. Lawson, et al. (2001). Aromatic interactions. *Journal of the Chemical Society, Perkin Transactions 25*, (651-669),1472-779X
- Hunter, C. A. and J. K. M. Sanders (1990). The nature of .pi.-.pi. interactions. *Journal of the American Chemical Society*,112,14, (5525-5534),0002-7863
- Ishikawa, Y., H. Yoshimi, et al. (1997). *Jpn. J. Appl. Phys., Part 1*,36,, (1233),
- Ju, S.-Y., J. Doll, et al. (2008). Selection of carbon nanotubes with specific chiralities using helical assemblies of flavin mononucleotide. *Nat Nano*,3,6, (356-362),1748-3387
- Ju, S. Y., W. P. Kopcha, et al. (2009). Brightly Fluorescent Single-Walled Carbon Nanotubes via an Oxygen-Excluding Surfactant Organization. *Science*,323,5919,(Mar) (1319-1323),0036-8075
- Ju, S. Y. and F. Papadimitrakopoulos (2008). Synthesis and redox behavior of flavin mononucleotide-functionalized single-walled carbon nanotubes. *Journal of the American Chemical Society*,130,2,(Jan) (655-664),0002-7863
- Kania, P. and P. Oelhafen (1995). Photoluminescence study of <100> textured CVD diamonds. *Diamond and Related Materials*,4,4, (425-428),0925-9635
- Karajanagi, S. S., H. Yang, et al. (2006). Protein-Assisted Solubilization of Single-Walled Carbon Nanotubes. *Langmuir*,22,4, (1392-1395),0743-7463
- Kim, K. S., Y. Zhao, et al. (2009). Large-scale pattern growth of graphene films for stretchable transparent electrodes. *Nature*,457,7230, (706-710),0028-0836
- Koga, K., G. T. Gao, et al. (2001). *Nature*,412,, (802),
- Li, J., H. T. Ng, et al. (2005). *Methods Mol. Bio.*,300, (191)
- Li, X., W. Cai, et al. (2009). Large-Area Synthesis of High-Quality and Uniform Graphene Films on Copper Foils. *Science*,324,5932,(June 5, 2009) (1312-1314)
- Li, X., W. Cai, et al. (2009). *Nano Lett.*,9, (4268-4272)
- Li, X., Y. Zhu, et al. (2009). *Nano Lett.*,9, (4359-4363)
- Lin, C. S., R. Q. Zhang, et al. (2005). Simulation of Water Cluster Assembly on a Graphite Surface. *The Journal of Physical Chemistry B*,109,29, (14183-14188),1520-6106

- Lin, C. S., R. Q. Zhang, et al. (2007). Geometric and Electronic Structures of Carbon Nanotubes Adsorbed with Flavin Adenine Dinucleotide: A Theoretical Study. *The Journal of Physical Chemistry C*,111,11, (4069-4073),1932-7447
- Liu, S., S. Gangopadhyay, et al. (1997). Photoluminescence studies of hydrogenated amorphous carbon and its alloys. *Journal of Applied Physics*,82,9, (4508-4514)
- Loginova, E., N. C. Bartelt, et al. (2008). *New J. Phys.*,10, (16)
- Loginova, E., N. C. Bartelt, et al. (2009). *New J. Phys.*,11, (20)
- Loh, K. P., J. S. Foord, et al. (1996). *Diamond Relat. Mater.*,5, (231)
- Malard, L. M., J. Nilsson, et al. (2007). Probing the electronic structure of bilayer graphene by Raman scattering. *Physical Review B*,76,20, (201401)
- Maniwa, Y., Y. Kumazawa, et al. (1999). *Jpn. J. Appl. Phys.*,38, (668)
- Mann, D. J. and M. D. Halls (2003). *Phys. Rev. Lett.*,90, (195503)
- Martí, J. and M. C. Gordillo (2001). *Phys. Rev. E*,64, (21504)
- Martí, J. and M. C. Gordillo (2003). *J. Chem. Phys.*,119, (12540)
- Martin, C. R. and P. Kohli (2003). The emerging field of nanotube biotechnology. *Nat Rev Drug Discov*,2,1, (29-37),1474-1776
- Mashl, R. J., S. Joseph, et al. (2003). *Nano Lett.*,3, (589)
- McCann, E. and V. I. Fal'ko (2006). Landau-Level Degeneracy and Quantum Hall Effect in a Graphite Bilayer. *Physical Review Letters*,96,8, (086805)
- McCarty, K. F., P. J. Feibelman, et al. (2009). *Carbon*,47, (1806)
- Mendes, R. C., E. J. Corat, et al. (1997). *Diamond Relat. Mater.*,6,, (490),
- Muehldorf, A. V., D. Van Engen, et al. (1988). Aromatic-aromatic interactions in molecular recognition: a family of artificial receptors for thymine that shows both face-to-face and edge-to-face orientations. *Journal of the American Chemical Society*,110,19, (6561-6562),0002-7863
- Nakada, K., M. Fujita, et al. (1996). Edge state in graphene ribbons: Nanometer size effect and edge shape dependence. *Physical Review B*,54,24, (17954)
- Nemanich, R. J., J. T. Glass, et al. (1988). Raman scattering characterization of carbon bonding in diamond and diamondlike thin films. *Journal of Vacuum Science & Technology A: Vacuum, Surfaces, and Films*,6,3, (1783-1787)
- Nevin, W. A., H. Yamagishi, et al. (1994). Emission of blue light from hydrogenated amorphous silicon carbide. *Nature*,368,6471, (529-531)
- Noon, W. H., K. D. Ausman, et al. (2002). *Chem. Phys. Lett.*,355, (445)
- Novoselov, K. S., A. K. Geim, et al. (2005). *Nature*,438, (197-200)
- Novoselov, K. S., A. K. Geim, et al. (2004). Electric Field Effect in Atomically Thin Carbon Films. *Science*,306,5696,(October 22, 2004) (666-669)
- Novoselov, K. S., D. Jiang, et al. (2005). *Proc. Natl. Acad. Sci. USA* 102, (10451-10453)
- Novoselov, K. S., E. McCann, et al. (2006). Unconventional quantum Hall effect and Berry's phase of  $2[\pi]$  in bilayer graphene. *Nat Phys*,2,3, (177-180),1745-2473
- Numata, M., M. Asai, et al. (2005). Inclusion of Cut and As-Grown Single-Walled Carbon Nanotubes in the Helical Superstructure of Schizophyllan and Curdlan ( $\beta$ -1,3-Glucans). *Journal of the American Chemical Society*,127,16, (5875-5884),0002-7863
- O'Connell, M. J., S. M. Bachilo, et al. (2002). Band Gap Fluorescence from Individual Single-Walled Carbon Nanotubes. *Science*,297,5581,(July 26, 2002) (593-596)
- Ohta, T., A. Bostwick, et al. (2006). Controlling the Electronic Structure of Bilayer Graphene. *Science*,313,5789,(August 18, 2006) (951-954)

- Ortiz-Acevedo, A., H. Xie, et al. (2005). Diameter-Selective Solubilization of Single-Walled Carbon Nanotubes by Reversible Cyclic Peptides. *Journal of the American Chemical Society*,127,26, (9512-9517),0002-7863
- Park, H. J., J. Meyer, et al. (2010). Growth and properties of few-layer graphene prepared by chemical vapor deposition. *Carbon*,48,4, (1088-1094),0008-6223
- Pender, M. J., L. A. Sowards, et al. (2005). Peptide-Mediated Formation of Single-Wall Carbon Nanotube Composites. *Nano Letters*,6,1, (40-44),1530-6984
- Pichon, A. (2008). Graphene synthesis: Chemical peel. *Nat Chem*,1755-4330
- Reina, A., X. T. Jia, et al. (2009). *Nano Lett.*,9, (30-35)
- Reina, A., S. Thiele, et al. (2009). *Nano Research*,2,6, (509-516)
- Robertson, J. (1995). Structural models of a-C and a-C:H. *Diamond and Related Materials*,4,4, (297-301)
- Robertson, J. (1996) (a). Photoluminescence mechanism in amorphous hydrogenated carbon. *Diamond and Related Materials*,5,3-5, (457-460)
- Robertson, J. (1996) (b). Recombination and photoluminescence mechanism in hydrogenated amorphous carbon. *Physical Review B*,53,24, (16302)
- Robertson, J. and E. P. O'Reilly (1987). Electronic and atomic structure of amorphous carbon. *Physical Review B*,35,6, (2946)
- Rusli, G. A. J. Amaratunga, et al. (1995). Photoluminescence in amorphous carbon thin films and its relation to the microscopic properties. *Thin Solid Films*,270,1-2, (160-164),0040-6090
- Saito, R., G. Dresselhaus, et al. (1998). *Physical Properties of Carbon Nanotube*,Imperial College Press,London
- Samarakoon, D. K. and X.-Q. Wang (2010). Tunable Band Gap in Hydrogenated Bilayer Graphene. *ACS Nano*,4,7, (4126-4130),1936-0851
- Sansom, M. S. P. and P. C. Biggin (2001). Biophysics: Water at the nanoscale. *Nature*,414,6860, (156-159),0028-0836
- Schütte, S., S. Will, et al. (1993). Electronic properties of amorphous carbon (a-C:H). *Diamond and Related Materials*,2,10, (1360-1364),0925-9635
- Silva, S. R. P., J. Robertson, et al. (1996). Structure and luminescence properties of an amorphous hydrogenated carbon. *Philosophical Magazine B: Physics of Condensed Matter; Statistical Mechanics, Electronic, Optical and Magnetic Properties*,74,4, (369-386)
- Sofo, J. O., A. S. Chaudhari, et al. (2007). Graphane: A two-dimensional hydrocarbon. *Physical Review B*,75,15, (153401)
- Stankovich, S., D. A. Dikin, et al. (2007). *Carbon*,45, (1558-1565)
- Starodub, E., S. Maier, et al. (2009). *Phys. Rev. B*,80, (8)
- Street, R. A. (1984). In: *Semiconductors and Semimetals*. J. I. Pankove,(Ed.). Vol. 84, (197), Academic Press New York.
- Su, Z., T. Leung, et al. (2006). Conformational Selectivity of Peptides for Single-Walled Carbon Nanotubes. *The Journal of Physical Chemistry B*,110,47, (23623-23627),1520-6106
- Sutter, P. W., J. I. Flege, et al. (2008). *Nat. Mater.*,7, (406-411)
- Thuvander, M. and H. O. Andréén APFIM Studies of Grain and Phase Boundaries: A Review. *Materials Characterization*,44,1-2, (87-100),1044-5803

- Tomásio, S. D. M. and T. R. Walsh (2007). Atomistic modelling of the interaction between peptides and carbon nanotubes. *Molecular Physics: An International Journal at the Interface Between Chemistry and Physics*,105,2, (221 - 229),0026-8976
- Tournus, F. and J. C. Charlier (2005). Ab initio study of benzene adsorption on carbon nanotubes. *Physical Review B*,71,16, (165421)
- Tournus, F., S. Latil, et al. (2005). pi -stacking interaction between carbon nanotubes and organic molecules. *Physical Review B*,72,7, (075431)
- Ugarte, D., T. Stoeckli, et al. (1998). *Appl. Phys. A.*,7, (101)
- Wagner, J. and P. Lautenschlager (1986). Hard amorphous carbon studied by ellipsometry and photoluminescence. *Journal of Applied Physics*,59,6, (2044-2047)
- Wakabayashi, K., M. Fujita, et al. (1999). Electronic and magnetic properties of nanographite ribbons. *Physical Review B*,59,12, (8271)
- Wang, J., Y. Zhu, et al. (2004). *Phys. Chem. Chem. Phys.*,6, (829)
- Wang, S., E. S. Humphreys, et al. (2003). Peptides with selective affinity for carbon nanotubes. *Nat Mater*,2,3, (196-200),1476-1122
- Wei, Z., D. Wang, et al. (2010). Nanoscale Tunable Reduction of Graphene Oxide for Graphene Electronics. *Science*,328,5984,(June 11, 2010) (1373-1376)
- Wu, J., W. Pisula, et al. (2007). Graphenes as Potential Material for Electronics. *Chemical Reviews*,107,3, (718-747),0009-2665
- Xu, S., M. Hundhausen, et al. (1993). Influence of substrate bias on the properties of a-C:H films prepared by plasma CVD. *Journal of Non-Crystalline Solids*,164-166,Part 2, (1127-1130),0022-3093
- Yu, Q., J. Lian, et al. (2008). Graphene segregated on Ni surfaces and transferred to insulators. *Applied Physics Letters*,93,11, (113103-113103)
- Zhang, Q., S. C. Bayliss, et al. (1996). The stable blue and unstable UV photoluminescence from carbon nanoclusters embedded in SiO<sub>2</sub> matrices. *Solid State Communications*,99,12, (883-886),0038-1098
- Zhang, R. Q., E. Bertran, et al. (1998). Size dependence of energy gaps in small carbon clusters: the origin of broadband luminescence. *Diamond and Related Materials*,7,11-12, (1663-1668),0925-9635
- Zhang, R. Q., T. S. Chu, et al. (2000). A Theoretical Study on the Interactions of Hydrogen Species with Various Carbon and Boron Nitride Phases. *The Journal of Physical Chemistry B*,104,29, (6761-6766),1520-6106
- Zhang, W. J., X. Jiang, et al. (1997). *J. Appl. Phys.*,82, (1896)
- Zhang, Y., T.-T. Tang, et al. (2009). Direct observation of a widely tunable bandgap in bilayer graphene. *Nature*,459,7248, (820-823),0028-0836
- Zheng, M., A. Jagota, et al. (2003). DNA-assisted dispersion and separation of carbon nanotubes. *Nat Mater*,2,5, (338-342),1476-1122
- Zheng, M., A. Jagota, et al. (2003). Structure-Based Carbon Nanotube Sorting by Sequence-Dependent DNA Assembly. *Science*,302,5650,(November 28, 2003) (1545-1548)
- Zorbas, V., A. Ortiz-Acevedo, et al. (2004). Preparation and Characterization of Individual Peptide-Wrapped Single-Walled Carbon Nanotubes. *Journal of the American Chemical Society*,126,23, (7222-7227),0002-7863



## **Physics and Applications of Graphene - Theory**

Edited by Dr. Sergey Mikhailov

ISBN 978-953-307-152-7

Hard cover, 534 pages

**Publisher** InTech

**Published online** 22, March, 2011

**Published in print edition** March, 2011

The Stone Age, the Bronze Age, the Iron Age... Every global epoch in the history of the mankind is characterized by materials used in it. In 2004 a new era in material science was opened: the era of graphene or, more generally, of two-dimensional materials. Graphene is the strongest and the most stretchable known material, it has the record thermal conductivity and the very high mobility of charge carriers. It demonstrates many interesting fundamental physical effects and promises a lot of applications, among which are conductive ink, terahertz transistors, ultrafast photodetectors and bendable touch screens. In 2010 Andre Geim and Konstantin Novoselov were awarded the Nobel Prize in Physics "for groundbreaking experiments regarding the two-dimensional material graphene". The two volumes *Physics and Applications of Graphene - Experiments* and *Physics and Applications of Graphene - Theory* contain a collection of research articles reporting on different aspects of experimental and theoretical studies of this new material.

### **How to reference**

In order to correctly reference this scholarly work, feel free to copy and paste the following:

R.Q. Zhang and Abir De Sarkar (2011). Theoretical Studies on Formation, Property Tuning and Adsorption of Graphene Segments, *Physics and Applications of Graphene - Theory*, Dr. Sergey Mikhailov (Ed.), ISBN: 978-953-307-152-7, InTech, Available from: <http://www.intechopen.com/books/physics-and-applications-of-graphene-theory/theoretical-studies-on-formation-property-tuning-and-adsorption-of-graphene-segments>

**INTECH**  
open science | open minds

#### **InTech Europe**

University Campus STeP Ri  
Slavka Krautzeka 83/A  
51000 Rijeka, Croatia  
Phone: +385 (51) 770 447  
Fax: +385 (51) 686 166  
[www.intechopen.com](http://www.intechopen.com)

#### **InTech China**

Unit 405, Office Block, Hotel Equatorial Shanghai  
No.65, Yan An Road (West), Shanghai, 200040, China  
中国上海市延安西路65号上海国际贵都大饭店办公楼405单元  
Phone: +86-21-62489820  
Fax: +86-21-62489821

© 2011 The Author(s). Licensee IntechOpen. This chapter is distributed under the terms of the [Creative Commons Attribution-NonCommercial-ShareAlike-3.0 License](#), which permits use, distribution and reproduction for non-commercial purposes, provided the original is properly cited and derivative works building on this content are distributed under the same license.

IntechOpen

IntechOpen